Wiley
Journal of Food Biochemistry
Volume 2025, Article ID 2952670, 19 pages
https://doi.org/10.1155/jfbc/2952670

WILEY

Research Article

Gardenia Fruit and Its Active Compound Crocin Protect Against Dexamethasone-Induced Muscle Atrophy via Nrf2 Activation

Jung-In Kim,[1,2] **Hang Yeon Jeong**,[1] **Young In Kim**,[1] **Ahyoung Yoo**,[1] **Hyunjung Lee**,[1] **Chang Hwa Jung**,[1,2] **and Jiyun Ahn**[1,2]

[1]*Aging Research Group, Korea Food Research Institute, Wanju-gun 55365, Jeollabuk-do, Republic of Korea*
[2]*Department of Food Biotechnology, University of Science and Technology, Wanju-gun 55365, Jeollabuk-do, Republic of Korea*

Correspondence should be addressed to Jiyun Ahn; jyan@kfri.re.kr

Received 18 December 2024; Revised 26 May 2025; Accepted 23 June 2025

Academic Editor: Miguel Rebollo-Hernanz

Copyright © 2025 Jung-In Kim et al. Journal of Food Biochemistry published by John Wiley & Sons Ltd. This is an open access article under the terms of the Creative Commons Attribution License, which permits use, distribution and reproduction in any medium, provided the original work is properly cited.

Background: Muscle mass gradually declines with age and the development of an effective strategy to prevent this is important. Gardenia fruit (*Gardenia jasminoides*; GJ), commonly used as a natural food colorant and in traditional herbal medicines, possesses antiinflammatory, antidiabetic, and antiangiogenic properties. However, its effects on muscle atrophy remain unexplored.
Purpose: In this study, we investigated the potential of GJ extract to mitigate dexamethasone (DEX)-induced muscle atrophy.
Methods: Cell experiments used C2C12 cells and myotube atrophy was induced with 50 μM DEX. Animal experiments used 7 week-old C57BL/6 mice and fed GJ at 0.05% or 0.1% in the diet for 8 weeks. DEX was injected intraperitoneally at 15 mg/kg per day for 18 days before dissection to induce muscle atrophy and the effects were evaluated.
Results: GJ enhanced myogenic differentiation by upregulating myogenic regulatory factors like *Myf5* and *MyoD* and inhibited DEX-induced myotube atrophy. Additionally, GJ reduced DEX-induced ROS production and mitochondrial dysfunction via Nrf2 activation. In mice, GJ protected the loss of muscle mass and decrease in muscle function by DEX. DEX-induced oxidative stress was reduced by GJ via the activation of Nrf2, followed by the transcription of antioxidant genes. HPLC analysis identified geniposide (GP) and crocin (CC) as the main constituents of GJ. However, only CC was found to exert antioxidant effects and effectively reduce DEX-induced oxidative stress and muscle atrophy via Nrf2 activation.
Conclusion: These findings suggest that GJ, particularly its bioactive component CC, may serve as a potential therapeutic agent for muscle atrophy.

Keywords: antioxidant activity; crocin; dexamethasone; *Gardenia jasminoides*; muscle atrophy; reactive oxygen species

1. Introduction

Skeletal muscle is an organ constituting approximately 40% of the human body weight and is composed of multinucleated cells known as muscle fibers [1]. However, muscle mass gradually declines at a rate of 1% per year from the age of 30 years onwards. Furthermore, in people over 60 years of age, muscle mass loss increases by ≥ 50% [2, 3], accompanied by a significant decrease in skeletal muscle strength; this condition is referred to as sarcopenia [4]. To date, a comprehensive understanding of the mechanisms underlying sarcopenia remains elusive; however, aging [5], abnormal reactive oxygen species (ROS) production [6], inflammation [7], and cachexia [8] have been implicated as potential causative factors. Moreover, muscle atrophy is characterized by a decrease in muscle mass, function, and cross-sectional area (CSA) [9].

Dexamethasone (DEX) is a synthetic glucocorticoid that is widely used to treat various inflammatory disorders, such as asthma [10], rheumatoid arthritis [11], and systemic lupus erythematosus [12], in humans. However, the long-term or high-dose use of DEX results in muscle atrophy as

a side effect [13]. DEX-induced muscle atrophy is caused by excessive ROS production [14]. To date, there is no FDA-approved drug for sarcopenia treatment. Hence, the development of an effective preventative strategy is imperative.

ROS are highly reactive molecules containing oxygen radicals [15]. The association between ROS and muscle atrophy includes several interrelated processes, such as oxidative stress and protein degradation [13]. Oxidative stress activates the ubiquitin–proteasome system in muscle cells, resulting in the degradation of damaged and unnecessary proteins, ultimately leading to a reduction in muscle mass and function [16, 17]. Intracellular ROS accumulation increases the expression of atrogenes [13]. Specifically, elevated ROS levels induce muscle atrophy by activating proteasome-dependent protein degradation through a muscle-specific increase in type E3 ubiquitin ligases, namely Atrogin-1 (MAFbx) and muscle-specific RING-finger protein-1 (MuRF1) [18]. Additionally, the primary site of ROS production is the mitochondrial electron transport system, which renders skeletal muscle more susceptible to ROS-induced damage than other tissues. Moreover, muscle atrophy is intricately linked to mitochondrial dysfunction, where excessive ROS production leads to oxidative damage [19].

Nuclear factor erythroid 2-related factor 2 (Nrf2) is a key regulator of cellular antioxidant defenses. Typically, Nrf2 is bound by Kelch-like ECH-associated protein 1 (Keap1) in the cytoplasm. Oxidative stress triggers Nrf2 release from Keap1, allowing Nrf2 to enter the nucleus, and activates genes with antioxidant response elements (AREs) that encode protective enzymes [20, 21]. The activation of Nrf2 is crucial for modulating oxidative stress, as it enhances the expression of various antioxidant enzymes, including catalase, superoxide dismutase (SOD), glutathione peroxidase, and heme oxygenase-1 (HO-1), which together neutralize ROS and restore cellular redox balance [22]. The absence of transcriptionally active Nrf2 is associated with muscle pathologies, such as muscle injury and atrophy [23]. Moreover, Nrf2 deficiency has been shown to accelerate muscle atrophy and induce a transition to fast-twitch muscle fibers in mice [24]. Thus, Nrf2 is considered a promising target for therapeutic intervention in muscle-wasting diseases.

Gardenia jasminoides (GJ) belongs to the Rubiaceae family, is native to Southeast Asia, and thrives in various regions of Asia [13]. Moreover, GJ fruit is extensively used as a natural food colorant in Asian countries. Its major constituents are crocin (CC), which produces a yellow color, and geniposide (GP), which produces a blue color [25]. GJ is associated with diverse biological activities, such as antiinflammatory, antidiabetic, and antiangiogenic effects [26]. However, its effects on muscle atrophy have not been investigated.

Therefore, in this study, we investigated the potential antioxidant and antimuscle wasting effects of GJ. Specifically, we examined how it influences muscle wasting and oxidative stress in the context of DEX-induced muscle atrophy using both a C2C12 cell model and experimental mouse model. To characterize the composition of GJ, HPLC analysis was further performed, and its functional compounds were identified.

2. Materials and Methods

2.1. Sample Preparation. Dried GJ (Imsil, Jeollabuk-do, South Korea) was obtained from South Korea and soaked in 50% ethanol (10 times the sample weight) at 80°C for 3 h. To obtain the GJ extract, the solution was filtered, concentrated, lyophilized, and stored. This procedure yielded 26.7% (w/w) of the extract (CC content ≥ 30 mg/g).

2.2. Cell Culture. Murine C2C12 myoblasts were sourced from the ATCC (Manassas, Virginia, USA) and cultured using 10% FBS (HyClone, Logan, Utah, USA)-containing DMEM (HyClone) for maintenance or 2% horse serum (HyClone)-containing DMEM for differentiation. Following a 4-day differentiation period, myotube atrophy was induced by adding 50 μM DEX (D4902, Sigma-Aldrich, St. Louis, Missouri, USA) with GJ or CC (PHL80391, Sigma-Aldrich) for 24 h. The separation of nuclear and cytoplasmic fractions was performed using NE-PER Nuclear and Cytoplasmic Extraction Reagents (78833, Thermo Scientific, Waltham, Massachusetts, USA). The Nrf2-specific inhibitor 5 μM ML385 (SML1833, Sigma-Aldrich) was cotreated with DEX in differentiated C2C12 cells for 24 h.

2.3. Cytotoxicity Assay. A 3-(4,5-dimethylthiazol-2-y1)-2,5-diphenyltetrazolium bromide (MTT; 475989, Sigma-Aldrich) assay was performed to evaluate cytotoxicity. The various concentrations of GJ, ranging from 0.1 to 10 μg/mL, or CC, ranging from 0.1 to 10 μM, were used to treat C2C12 cells for 24 h. Then, 0.5 mg/mL MTT solution was added for 4 h. The insoluble formazan was dissolved in dimethyl sulfoxide (DMSO; D5879, Sigma-Aldrich), and the 96-well plate (30096, SPL, Pocheon, Gyeonggi-do, South Korea) with the solution was measured at 570 nm.

2.4. Immunohistochemistry Analysis. For immunofluorescence staining to detect myosin heavy chain (MHC), myotubes were incubated with an anti-MHC mouse monoclonal antibody (MF20; DSHB, Iowa City, Iowa, USA). The fusion index was measured as previously described [27]. To assess the myotube diameter, the microscopic fields (Olympus IX71, Olympus Corporation, Tokyo, Tokyo, Japan) were selected at random from the 6-well plates (30006, SPL); the diameter was measured at three different positions for at least 100 myotubes in each well. The mean of three measurements was used to determine the average diameter of the myotubes.

2.5. Quantitative Reverse-Transcription PCR (qRT-PCR). Total RNA was extracted using the NucleoSpin RNA II kit (Macherey-Nagel, Düren, North Rhine-Westphalia, Germany), and cDNA synthesis was performed. qRT-PCR was performed using a ViiA7 system (Applied Biosystems, Foster

City, California, USA) and SYBR Green (TOYOBO Co., Ltd., Osaka, Osaka, Japan). The primers used are listed in Table S1.

2.6. Western Blot Analysis. Differentiated C2C12 cells and skeletal muscle tissue were lysed as described previously [13]. After sodium dodecyl sulfate–polyacrylamide gel electrophoresis, proteins were transferred to a polyvinylidene difluoride membrane (Thermo Scientific). The membranes were incubated with antibodies to assess protein expression. Each antibody was purchased as follows: total MHC (MF-20) from DSHB; MuRF1 (ab183094), catalase (ab16731), and SOD1 (ab13498) from Abcam Inc. (Cambridge, Cambridgeshire, UK); vinculin (V9131) from Sigma-Aldrich; Keap1 (8047S) and TATA-binding protein (TBP; 8515) from Cell Signaling Technology Inc. (Danvers, Massachusetts, USA); β-actin (sc-47778) and Atrogin-1 (sc-166806) from Santa Cruz Biotechnology Inc. (Dallas, Texas, USA); and Nrf2 (NBP1-32822), HO-1 (NBP1-31341), and NAD(P)H: quinone oxidoreductase 1 (NQO1; NB200-209) from Novus Biologicals (Centennial, Colorado, USA). Chemiluminescent reagent (Bio-Rad Laboratories, Hercules, California, USA) treatment enabled visualization of immunoreactive proteins. Images were captured using a G:BOX Chemi XX6 (Syngene Ltd., Frederick, Maryland, USA).

2.7. 1,1-Diphenyl-2-Picrylhydrazyl (DPPH)-Scavenging and $ABTS^+$ Radical-Scavenging Activity. The scavenging activity of DPPH (0.2 mM, Abcam Inc.) was spectrophotometrically determined. The GJ, CC, and GP (SML0153, Sigma-Aldrich) were mixed with DPPH solution. The solutions were then incubated at 25°C, and the absorbance was measured at 517 nm. For the $ABTS^+$ (Sigma-Aldrich) assay, a solution containing $ABTS^+$ radicals was mixed with a 7 mM ABTS solution containing 2.5 mM potassium persulfate (at a ratio of 95:5, v/v) and incubated for 12 h at 4°C in the absence of light. A mixture was prepared comprising 198 μL of the solution with 2 μL of GJ, and the absorbance was determined at 735 nm.

2.8. Detection of Intracellular ROS Levels. Intracellular ROS generation was assessed using dichlorodihydrofluorescein diacetate (DCF-DA; Molecular Probes, Eugene, Oregon, USA). To measure mitochondrial superoxide production, 5 μM of MitoSOX Red (Molecular Probes) was added to the cells, followed by incubation for 20 min. Mitochondrial subcellular localization was confirmed through colabeling with 50 nm MitoTracker Green FM (Molecular probes).

2.9. Measurement of Oxygen Consumption Rate (OCR). The OCR was measured using an XF94 Extracellular Flux Analyzer and an XF Cell Mito Stress Test Kit (Seahorse Bioscience, Billerica, Massachusetts, USA). C2C12 cells were seeded onto XF-94 microplates and incubated for 24 h. GJ or CC was added with 50 μM DEX, followed by incubation for 24 h. After replacing the cell medium containing 25 mM glucose, 1 mM pyruvate, and 1 mM glutamine, the cells were maintained in 5% CO_2 at 37°C for 1 h. The injection port was then filled with oligomycin A (1.5 μM), carbonyl cyanide-4-(trifluoromethoxy) phenylhydrazone (4 μM), and antimycin A (1 μM).

2.10. Animals. Six-week-old male C57BL/6 mice (Orient Bio, Seongnam, Gyeonggi-do, South Korea) were housed at an environment of 21°C–23°C with a 12-h light/dark cycle. After 1 week of adaptation, 40 mice were randomly divided into four groups ($n = 10$/group), as follows: Group I, phosphate-buffered saline injection (Con group); Group II, water-soluble DEX (D2915, Sigma-Aldrich) injection (DEX group); Group III, DEX injection and 0.05% GJ supplementation (GJL group); Group IV, DEX injection and 0.1% GJ supplementation (GJH group). For 8 weeks, mice were fed the AIN-93M diet (Research Diets, Inc., New Brunswick, NJ, USA) supplemented with or without 0.05% or 0.1% GJ for 8 weeks, corresponding to human-equivalent doses of 50 mg/kg and 100 mg/kg, respectively. Since a previous study reported no toxicity at doses of 440 mg/kg and 880 mg/kg, we selected lower doses [28]. For the last 18 days, DEX (15 mg/kg/day) was injected intraperitoneally to induce muscle atrophy. After 8 weeks, the mice were euthanized using 5% isoflurane, and muscle tissues were acquired for further analysis. No mortality or clinical signs were observed during the experimental period. All animal experiments were performed according to the guidelines of the Korea Food Research Institute Institutional Animal Care and Use Committee (KFRI-M-19034).

2.11. Measurement of Muscle Performance. To evaluate the grip strength of the forelimbs, the mice were subjected to three trials using a grip strength test (Bioseb, Vitrolles, Provence-Alpes-Côte d'Azur, France). The endurance running test was performed using a motorized speed-controlled modular rodent treadmill system (Ugo Basile, Varese, Lombardy, Italy) equipped with an electronic shock stimulus grid. All mice were subjected to a 2-day acclimation period of running on a treadmill. On the first day of adaptation, the mice ran at a speed of 5 m/min for 10 min and then at 10 m/min for an additional 10 min. On the second day, the mice were subjected to a 15° incline and ran at 5 m/min for 5 min and then at 10 m/min for 15 min. After this 2-day adaptation period, the mice ran with an incline of 15° for 20 min at 10 m/min, and then, the speed was increased every 2 min up to 20 m/min until exhaustion. The wire-hanging test was also conducted by placing a mouse on a wire and recording the time it took to fall onto a sponge on the floor. For footprint analysis, we trained the mice to walk on filter paper along a 100-cm-long and 6-cm-wide runway the day before the experiment. Blue nontoxic paint was applied to the hind paws, and red paint was applied to the front paws. Stride lengths based on the front and hind paws were determined by measuring the average forward distance between each stride.

2.12. Body Composition Analysis. Body composition analysis was performed using a dual-energy X-ray absorptiometry (DXA) with an InAlyzer system (Medikors Co., Seongnam,

Gyeonggi-do, South Korea). The mice were placed in the prone position on the scanner bed, extending their limbs and tails away from their bodies, as per the operational instructions. After scanning, the InAlyzer software (Medikors Co.) was used to calculate fat and lean body masses.

2.13. Histological Analysis. Gastrocnemius muscle sections were cut at 7-μm intervals using a cryomicrotome (Leica Microsystems, Wetzlar, Hesse, Germany). Skeletal muscle tissue sections were fixed in refrigerated 20% acetone and blocked with 10% FBS (Hyclone). The tissues were then exposed to laminin antibody (NB-300, NOVUS Biologicals) overnight. MHC1 (BA-F8), MHC2A (SC-71-C), and MHC2B (BF-F3) antibodies (DSHB) were used to measure the muscle-type transition. The tissues were fixed with fluoroshields (F6182, Sigma-Aldrich), and images were captured using a confocal microscope (Digital Eclipse C1 Plus, Nikon, Tokyo, Tokyo, Japan).

2.14. Antioxidant Activity Measurement. An equivalent amount of quadriceps protein was used for the measurements. SOD activity was assessed using an assay kit (ab65354, Abcam). Glutathione peroxidase activity and muscle malondialdehyde (MDA) levels were measured using an assay kit (ab102530, Abcam) and ELISA kit (MBS741034, MyBioSource, Inc., San Diego, California, USA), respectively.

2.15. HPLC Analysis. HPLC analysis was performed using JASCO liquid chromatography (JASCO, Tokyo, Tokyo, Japan) with a CAPCELL PAK C18 MG II S-5 (4.6 mm × 250 mm, 4.3 μm, YMC Co. Ltd., Kyoto, Kyoto, Japan) and an MD-2010 Plus DAD detector (JASCO). The mobile phase consisted of solvent A, water with 1% acetic acid (Junsei, Tokyo, Tokyo, Japan), and solvent B, 100% acetonitrile (J. T. Baker, Philipsburg, New Jersey, USA). The gradient program started with a 90:10 A/B ratio and switched to a 75:25 A/B ratio in 5 min. Following this phase, the gradient was maintained at a 75:25 A/B ratio from 5 to 20 min, switched to 5:95 at 25 min, and continued until 30 min. The flow rate was 1.0 mL/min, the injection volume of the sample was 10 μL, and the temperature of the column oven was kept at 40°C. CC (PHL80391, Sigma-Aldrich, PubChem CID 5281233) was detected at a wavelength of 450 nm, whereas GP (SML0153, Sigma-Aldrich, PubChem CID 107848), chlorogenic acid (PHL89175, Sigma-Aldrich, PubChem CID 1794427), geniposidic acid (SMB00441, Sigma-Aldrich, PubChem CID 443354), and genipin (G4796, Sigma-Aldrich, PubChem CID 442424) were detected at a wavelength of 254 nm. The standard calibration curves for CC, GP, chlorogenic acid, geniposidic acid, and genipin are presented in Figure 1S.

2.16. Statistical Analysis. Data are shown as the mean ± SD and mean ± SEM for cell-based and animal studies, respectively. Statistical analyses were performed using GraphPad Prism 9 software (San Diego, California, USA). The Bonferroni post hoc test was conducted if the ANOVA revealed significance ($p < 0.05$).

3. Results

3.1. GJ Promotes Myogenesis and Inhibits DEX-Induced Atrophy in C2C12 Cells. First, we evaluated whether GJ could be used as a functional material to mitigate the muscle atrophy in C2C12 cells. The MTT assay demonstrated greater than 90% cell viability at concentrations of ≤ 10 μg/mL GJ (Figure 1(a)). Moreover, GJ treatment during myogenic differentiation resulted in a concentration-dependent increase in the fusion index compared with that in the Con (Figures 1(b), 1(c)). Furthermore, the expression levels of muscle differentiation markers, such as *Myf5* and *MyoD*, were upregulated in a concentration-dependent manner (Figures 1(d), 1(e)). These results suggest that GJ increases myogenic differentiation in C2C12 myoblasts.

An examination of the protective effect of GJ against myotube atrophy showed that DEX-induced myotube atrophy in C2C12 myotubes was effectively inhibited by GJ (Figures 1(f), 1(g)). qRT-PCR analysis further showed that DEX treatment increased the expression of *Atrogin-1, MuRF1*, and *myostatin* and decreased expression of the myogenic factors *MyoG* and *MyoD*; however, these changes were reversed after GJ treatment (Figure 1(h)). Western blot analysis confirmed that GJ treatment increased total MHC protein expression, which was diminished after DEX treatment (Figures 1(i), 1(j)). These results indicate that GJ inhibits DEX-induced muscle atrophy in C2C12 myotubes.

3.2. GJ Attenuates DEX-Induced Oxidative Stress and Mitochondrial Dysfunction via Activation of Nrf2. To measure the antioxidant activity of GJ, we conducted DPPH and $ABTS^+$ radical-scavenging assays and found that GJ treatment results in a concentration-dependent increase in antioxidant activity (Figures 2(a), 2(b)). Moreover, the DCF-DA assay showed that treatment with DEX increased the DCF fluorescence intensity, and cotreatment with GJ suppressed these levels (Figures 2(c), 2(d)). We then measured mitochondrial oxidative stress using MitoSOX and observed that GJ significantly decreased MitoSOX fluorescence (Figures 2(e), 2(f)). These results suggested that GJ effectively attenuates DEX-induced oxidative stress in differentiated myotubes.

Next, we determined the effect of GJ on mitochondrial respiration. DEX treatment significantly reduced the OCR for basal, maximal, and spare respiration, as well as ATP production (Figures 2(g), 2(h)). Cotreatment with GJ inhibited the DEX-induced decrease in mitochondrial respiration. To examine whether GJ induces the activation of Nrf2, we measured the translocation of Nrf2 from the cytosol and to the nucleus. For this, cytosolic and nuclear fractions were isolated from C2C12 cells treated with GJ. Western blot analysis was performed to determine the levels of Nrf2 in these fractions (Figures 2(i), 2(j)). Treatment with DEX increased cytoplasmic Nrf2 levels and decreased nuclear Nrf2 levels, indicating that Nrf2 translocation to the nucleus was reduced under DEX-induced stress conditions. However, treatment with GJ decreased Nrf2 levels in the cytoplasm and increased them in the nucleus compared to DEX, suggesting that GJ promotes Nrf2 translocation to the nucleus, thereby enhancing its antioxidant capacity.

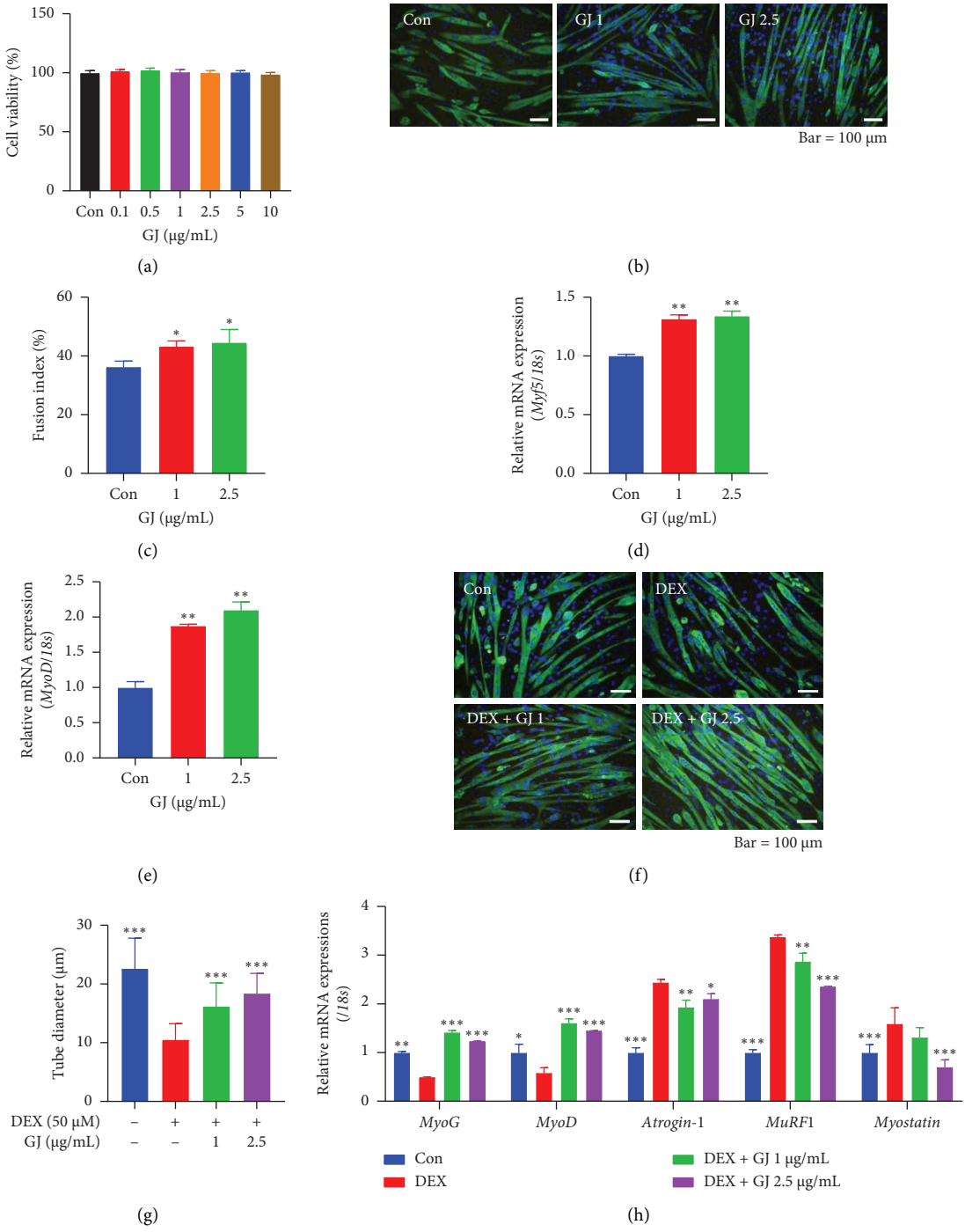
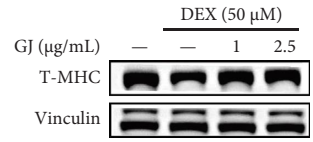
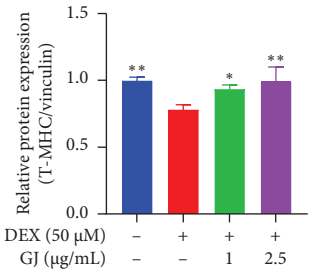


Figure 1: Continued.



(i)



(j)

Figure 1: GJ promotes myogenic differentiation and inhibits DEX-induced myotube atrophy. (a) Effect of GJ on cell viability. After treatment of various concentrations of GJ for 24 h, cell viability was measured by MTT assay. (b) Immunofluorescence (IF) staining of myosin heavy chain (MHC) in differentiated C2C12 myotubes in the presence or absence of GJ for 4 days. (c) The fusion index (%) for immunofluorescence staining was calculated. (d), (e) The mRNA expression of myogenic regulatory factors, including *Myf5* (d) and *MyoD* (e), was measured by qRT-PCR. Data are means ± SD. $^{*}p < 0.05$ and $^{**}p < 0.01$ versus Con. (f) After cotreatment of DEX and GJ for 24 h, IF staining of MHC was performed in C2C12 myotubes. (g) Quantification of C2C12 myotube diameter. (h) Measurements of mRNA expression involved in myogenesis (*MyoG* and *MyoD*) and muscle atrophy (*Atrogin-1, MuRF1,* and *myostatin*) in DEX- and GJ-cotreated C2C12 myotubes. (i) Western blotting analysis for total MHC in DEX- and GJ-cotreated C2C12 myotubes. (j) Quantification of protein bands of (i). Data are means ± SD. $^{*}p < 0.05$, $^{**}p < 0.01$, $^{***}p < 0.001$ versus DEX.

A measurement of antioxidant-associated protein expression using Western blot analysis to assess the effect of GJ on redox signaling showed that DEX treatment induced a decrease in Nrf2 expression owing to a decrease in the degradation of Keap1. The suppression of Nrf2 mediated by Keap1 was attenuated by GJ, leading to the increased expression of antioxidant genes, such as HO-1, NQO1, SOD1, and catalase (Figures 2(k), 2(l)). These results indicate that GJ inhibits DEX-induced oxidative stress by regulating the Nrf2/Keap1 antioxidant pathway in differentiated myotubes.

3.3. Dietary GJ Improves Muscle Function During DEX-Induced Muscle Atrophy. We investigated whether GJ supplementation could prevent DEX-induced muscle atrophy in mice (Figure 3(a)). Eight weeks of GJ supplementation did not alter body weight or induce pathological lesions in any organs (Figure 3(b)). A measurement of the grip strength showed that the DEX-induced decrease in muscle strength was effectively prevented by GJ supplementation (Figure 3(c)). Moreover, measurements of the physical performance using treadmill, wire-hanging, and stance tests showed that the DEX group exhibited a decrease in exercise performance compared with that in the Con group, whereas the GJ-supplemented groups exhibited concentration-dependent recovery (Figures 3(d), 3(e), 3(f)). These results confirmed that GJ increases muscle strength and improves physical performance in mice after DEX-induced muscle atrophy.

3.4. Dietary GJ Attenuates Muscle Loss During DEX-Induced Muscle Atrophy. The effects of dietary GJ supplementation on muscle mass during DEX-induced muscle atrophy were investigated by analyzing the mouse body composition using DXA. This revealed an increase in the lean body mass and a decrease in the fat mass following GJ supplementation (Figures 4(a), 4(b), 4(c)). The skeletal muscle weight, which was measured after dissection, was significantly reduced in the DEX group relative to that in the Con group; however, GJ supplementation increased the skeletal muscle weight, particularly that of the quadriceps and gastrocnemius muscles (Figure 4(d)).

A further histological analysis of the gastrocnemius muscle, to confirm the alterations within the muscle tissue, showed that the CSA decreased by approximately 47% in the DEX group compared with that in the Con group but was significantly increased following GJ supplementation (Figures 4(e), 4(f)). An analysis of muscle fiber-type transitions showed that GJ supplementation shifted the myofiber size distribution to the right, suggesting the presence of more myofibers with a larger CSA, compared to observations in the DEX group (Figure 4(g)). Immunofluorescence staining of MHC isotypes demonstrated that the DEX injection caused a shift toward reduced proportions of type 2 muscle fibers, whereas GJ effectively reversed the DEX-induced alterations in the muscle fiber composition (Figures 4(h), 4(i), 4(j)). These results suggest that GJ supplementation mitigates muscle loss and alterations in the muscle fiber composition during DEX-induced muscle atrophy.

3.5. Dietary GJ Reduces DEX-Induced Muscle Atrophy via Antioxidant Activity and Nrf2 Activation. Given the significant increase in muscle mass and function induced by GJ, we measured the protein expression of total MHC and atrogenes in the gastrocnemius muscle tissues. Western blot analysis revealed that GJ reversed DEX-induced reduction in total MHC. GJ also decreased the protein levels of Atrogin-1(Figures 5(a), 5(b)). To further elucidate the potential role of GJ in enhancing the antioxidant activity in muscle tissues, we assessed oxidative stress-related enzyme activities and lipid peroxide levels in gastrocnemius muscles. The activity of two crucial antioxidant enzymes, SOD and glutathione peroxidase, was reduced in the muscle tissue injected with DEX alone, but this was recovered considerably in the GJ groups (Figures 5(c), 5(d)). The muscle tissue concentration

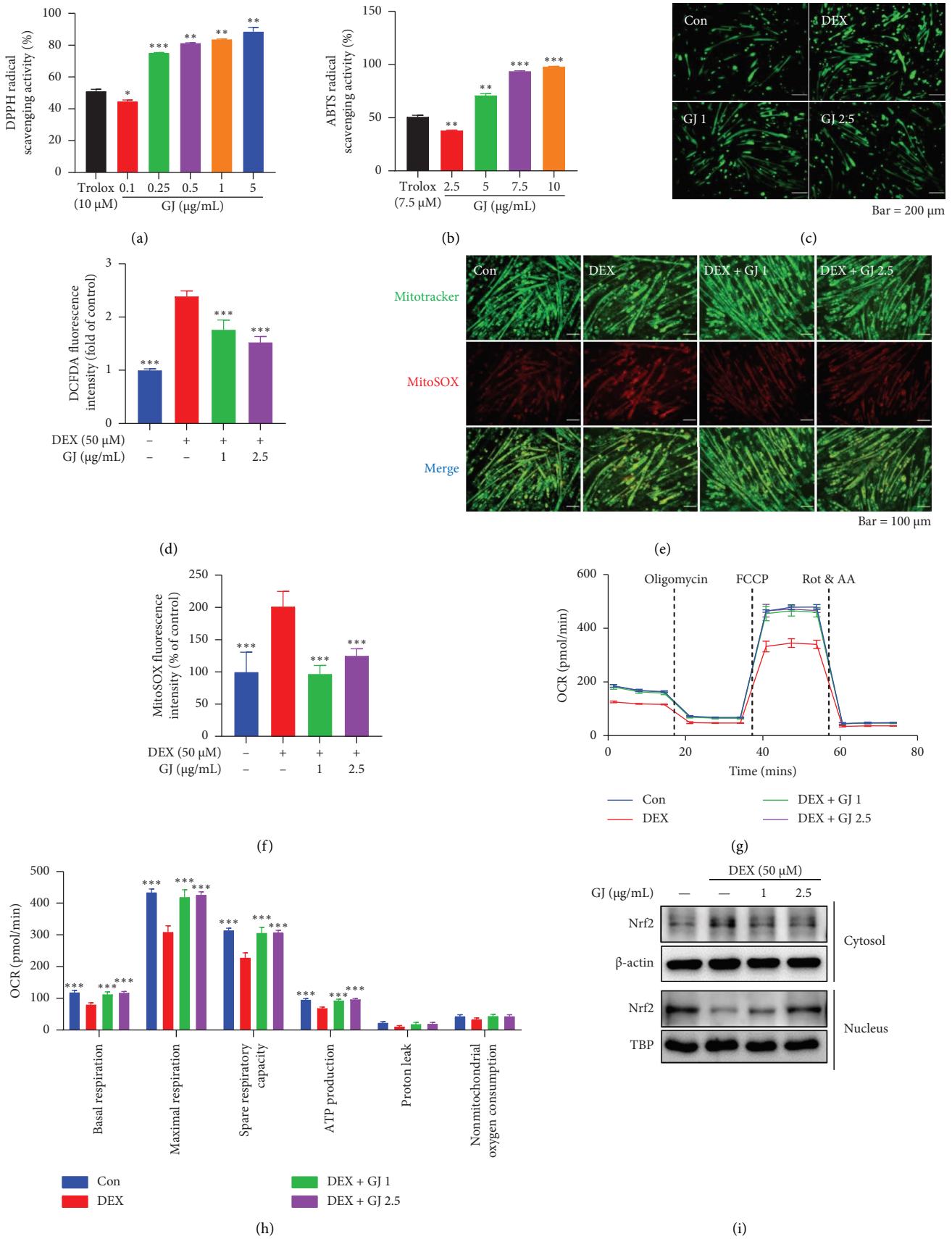


Figure 2: Continued.

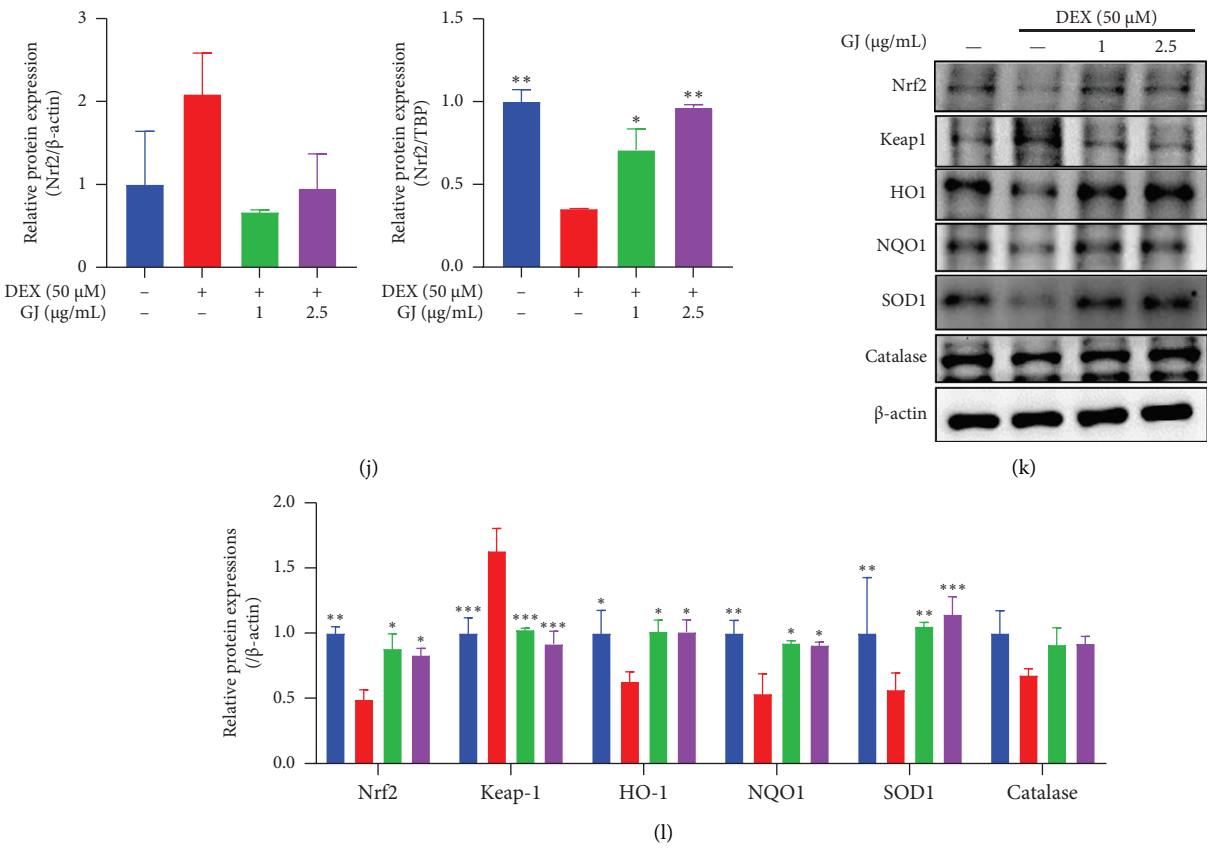


Figure 2: Antioxidant activity of GJ attenuates DEX-induced oxidative stress in C2C12 myotubes. (a) Antioxidant activity of GJ by DPPH assay. (b) Antioxidant activity of GJ by ABTS assay. Data are means ± SD. $^{*}p < 0.05$, $^{**}p < 0.01$, $^{***}p < 0.001$ versus Trolox. (c) Intracellular ROS was measured by DCF-DA staining after cotreatment of DEX and GJ in C2C12 myotubes. (d) The DCF fluorescence intensity in C2C12 myotubes. (e) MitoTracker Green and MitoSOX Red stainings were performed in C2C12 myotubes. (f) Quantification of fluorescent intensity of MitoSOX Red staining. (g) Mitochondrial respirometry analysis using XF96 analyzer to measure mitochondrial OCR. (h) Quantification of mitochondrial respiration. (i) Measurement of nuclear translocation of Nrf2 in C2C12 cells. (j) Quantification of protein bands of (i). (k) Western blot analysis of Nrf2 and its downstream targets. (l) Quantification of protein bands of (k). Data are means ± SD. $^{*}p < 0.05$, $^{**}p < 0.01$, $^{***}p < 0.001$ versus DEX.

of MDA was notably higher in the DEX-injected group compared to the Con group, but the levels in the GJL and GJH groups were comparable to those in the Con group (Figure 5(e)). Furthermore, an analysis of antioxidant-associated protein expression revealed that dietary GJ significantly increased the expression of Nrf2 and its downstream targets, HO-1 and NQO1. In contrast, GJ decreased Keap-1 expression (Figures 5(f), 5(g)). These findings suggest that GJ intake ameliorates muscle atrophy by augmenting antioxidant activity in the muscle tissue. To confirm that GJ ameliorates muscle atrophy via Nrf2 activation, we cotreated C2C12 myotubes with ML385, a specific Nrf2 inhibitor, along with DEX and GJ. We observed that DEX treatment decreased the diameter of the myotubes, while simultaneous treatment with GJ and DEX restored the myotube diameter. However, this protective effect of GJ was abolished by ML385 treatment (Figures 5(h), 5(i)). Furthermore, we assessed the expression levels of *Atrogin-1* and *MuRF1* (Figure 5(j)). DEX treatment led to the upregulation of both *Atrogin-1* and *MuRF1*. Furthermore, at the protein level, we found that the GJ-induced increase in expression of SOD1 and catalase, which are regulated by Nrf2, tended to be reduced by ML385 treatment (Figures 5(k), 5(l)). This upregulation was substantially suppressed by GJ treatment, which is consistent with its protective role against muscle atrophy. However, the inhibitory effect of GJ was abrogated in the presence of ML385, indicating that Nrf2 plays a crucial role in mediating the anti-muscle-wasting effects of GJ. Overall, these results suggest that the efficacy of GJ in mitigating DEX-induced muscle atrophy is mediated by Nrf2 activation.

3.6. HPLC Analysis of GJ. The quantitative analysis of bioactive compounds in GJ was performed using HPLC to measure the concentration of five major compounds, namely genipin, GP, geniposidic acid, CC, and chlorogenic acid. The chromatograms of the compounds in GJ are shown (Figures 6(a), 6(b)). The results showed that the concentrations of GP and CC in GJ were 135.36 ± 1.55 and 30.34 ± 0.97 mg/g extract, respectively (Table 1). In our previous study, we reported the protective effect of GP on DEX-induced muscle atrophy [29]. Thus, we examined whether CC contributes to the protective effect of GJ against muscle atrophy.

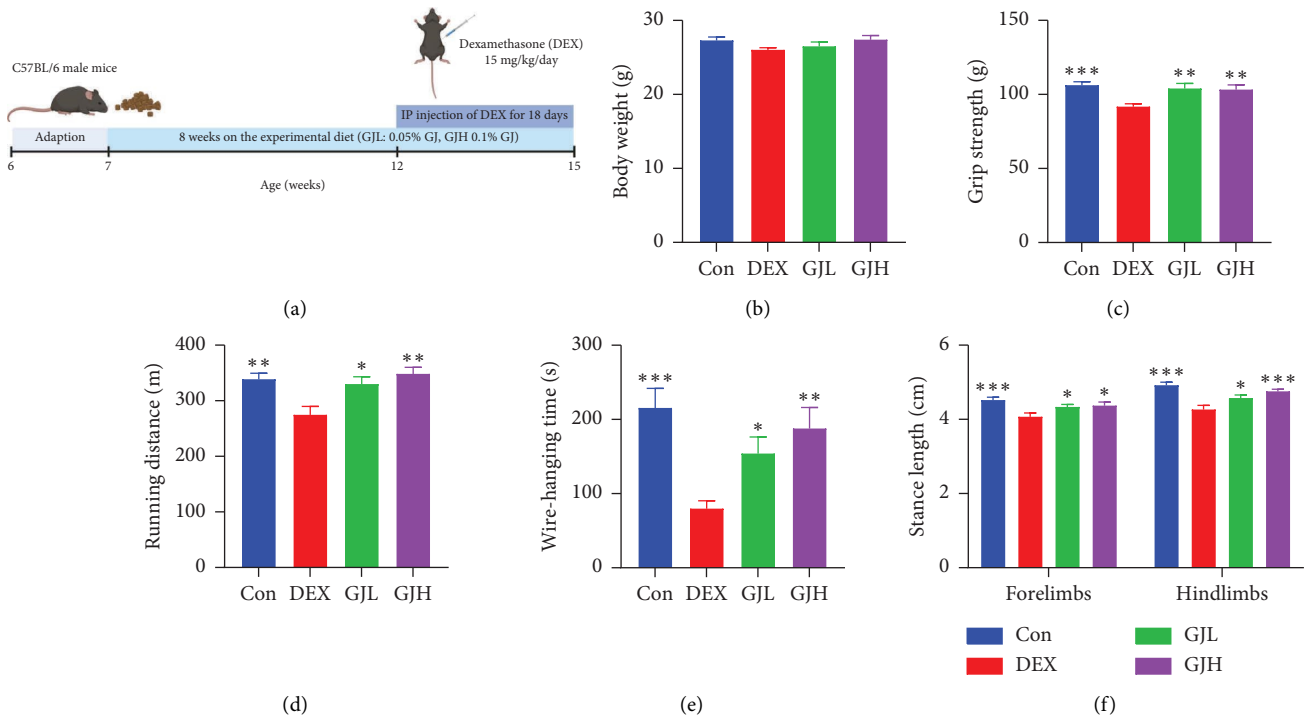


FIGURE 3: GJ supplementation improves muscle function and physical performance exercise performance in DEX-induced muscle atrophy in mice. (a) Schematic representation of animal experiment (DEX injection and 0.05% GJ supplementation: GJL, DEX injection, and 0.1% GJ supplementation: GJH). (b) Final body weight. (c) Muscle function by grip strength test. (d) Total running distance measured by treadmill test. (e) Wire-hanging time by hanging test. (f) Measurement of stance length. Data are means ± SEM. $^{*}p < 0.05$, $^{**}p < 0.01$, $^{***}p < 0.001$ versus DEX.

3.7. The Antioxidant CC Improves DEX-Induced Myotube Atrophy. A comparison of the DPPH radical-scavenging activity between the two major GJ components showed that CC exhibited a concentration-dependent increase in antioxidant activity, whereas GP showed no antioxidant activity (Figure 7(a)). Therefore, we investigated the preventive effects of CC on DEX-induced oxidative stress. CC did not affect the viability of C2C12 cells at concentrations up to 10 μM (Figure 7(b)). Moreover, at a nontoxic concentration, CC treatment significantly reduced the DEX-induced accumulation of intracellular ROS (Figures 7(c), 7(d)). Additionally, mitochondrial ROS accumulation was significantly decreased following CC treatment (Figures 7(e), 7(f)). A measurement of the effect of CC on mitochondrial respiration also showed that CC effectively ameliorated DEX-induced mitochondrial dysfunction (Figures 7(g), 7(h)). In addition, an analysis of the alterations in antioxidant-associated protein expression revealed that CC treatment increased Nrf2 expression and decreased Keap1 expression. Furthermore, CC treatment increased the expression of Nrf2-target genes and antioxidant enzymes (Figures 7(i), 7(j)). These results indicated that CC attenuates DEX-induced oxidative stress in myotubes.

Finally, we determined whether this decrease in oxidative stress leads to the inhibition of muscle atrophy. CC treatment effectively decreased DEX-induced myotube atrophy (Figures 7(k), 7(l)) and inhibited the DEX-induced decrease in total MHC levels, as well as the increase in atrophy marker levels (Figures 7(m), 7(n)). In the comparative in vitro differentiation assay, CC showed a lower effect on promoting differentiation compared to GJ, suggesting that the combination treatment enhances differentiation. However, in the DEX-induced myotube atrophy model, both GJ and CC exhibited comparable protective effects. These results indicate that CC is a major compound responsible for the anti-atrophic effect of GJ (Figure 2S). These findings suggest that the inhibitory effects of GJ on muscle atrophy could be partially mediated by CC.

4. Discussion

Increased ROS production in skeletal muscles contributes to muscle atrophy through dysregulated proteolysis [13]. Thus, reducing oxidative stress could be an effective preventive strategy to reduce muscle atrophy. This study provides evidence that GJ ameliorates DEX-induced muscle atrophy by decreasing ROS production and improving mitochondrial function via Nrf2 activation. Moreover, CC, which is a carotenoid found in GJ, was suggested to be one of the functional components of GJ that prevents muscle atrophy.

The evidence regarding the preventive effect of dietary antioxidants on sarcopenia remains controversial. Accumulated data have reported that the intake of antioxidants such as vitamins, carotenoids, and vegetables/fruits prevents or ameliorates sarcopenia by eliminating ROS. In contrast, Mediterranean dietary patterns, which are rich in antioxidants, are not related to the low incidence of sarcopenia.

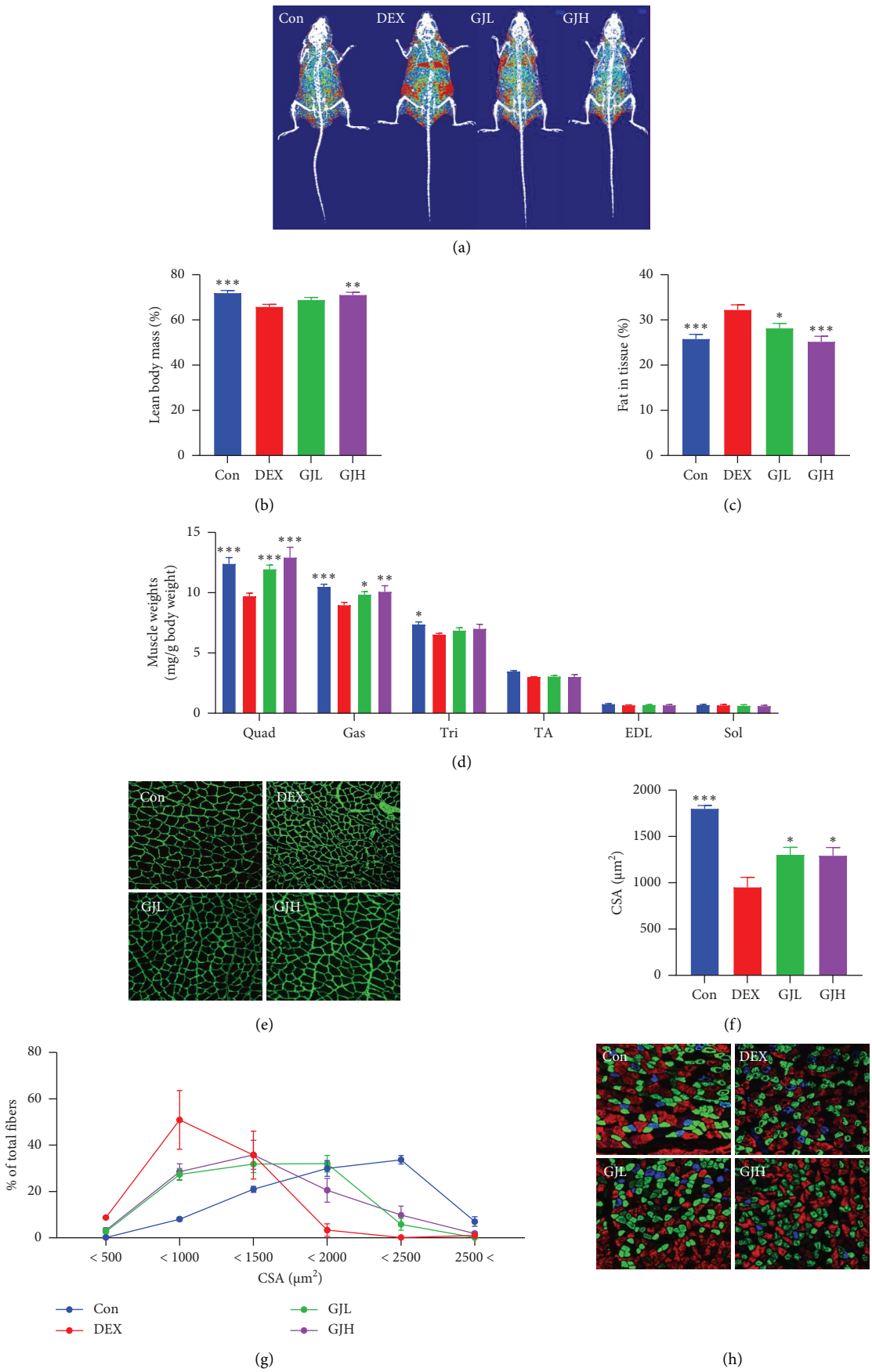


Figure 4: Continued.

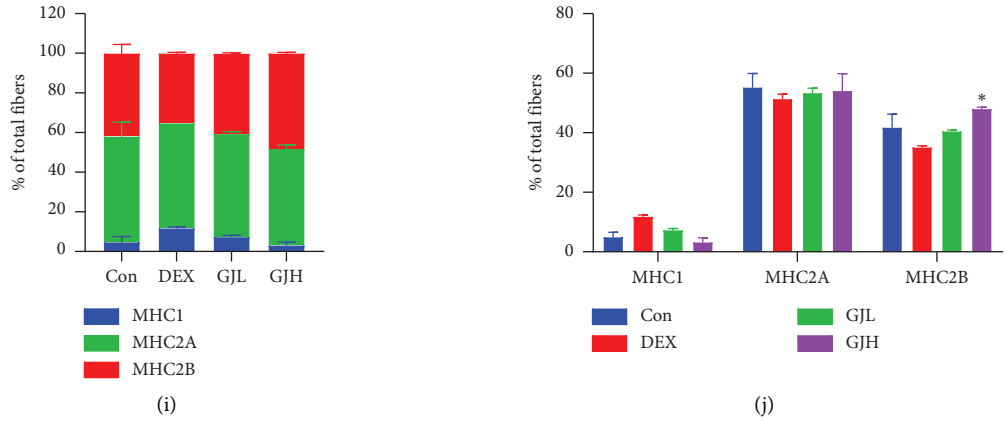


Figure 4: GJ supplementation prevents muscle loss in DEX-induced muscle atrophy in mice. (a) Representative DXA scan images. (b) Lean body mass (%). (c) Body fat percentage (%). (d) Skeletal muscle weights were normalized to body weights. Quad: Quadriceps; Gas: Gastrocnemius; Tri: triceps brachii; TA: tibialis anterior; EDL: extensor digitorum longus. (e) IF staining of laminin in gastrocnemius muscle. (f) The mean CSA values for GAS muscle tissues. (g) The distribution of CSA in gastrocnemius muscle. (h) Triple IF staining for MHC1 (blue, type 1 fibers), MHC2A (green, type 2A fibers), and MHC2B (red, type 2b fibers). (i) The proportion of MHC isoforms-specific fibers according to experimental groups. (j) The percentage of MHC isoforms-specific fibers. Data are means ± SEM. $^{*}p < 0.05$, $^{**}p < 0.01$, $^{***}p < 0.001$ versus DEX.

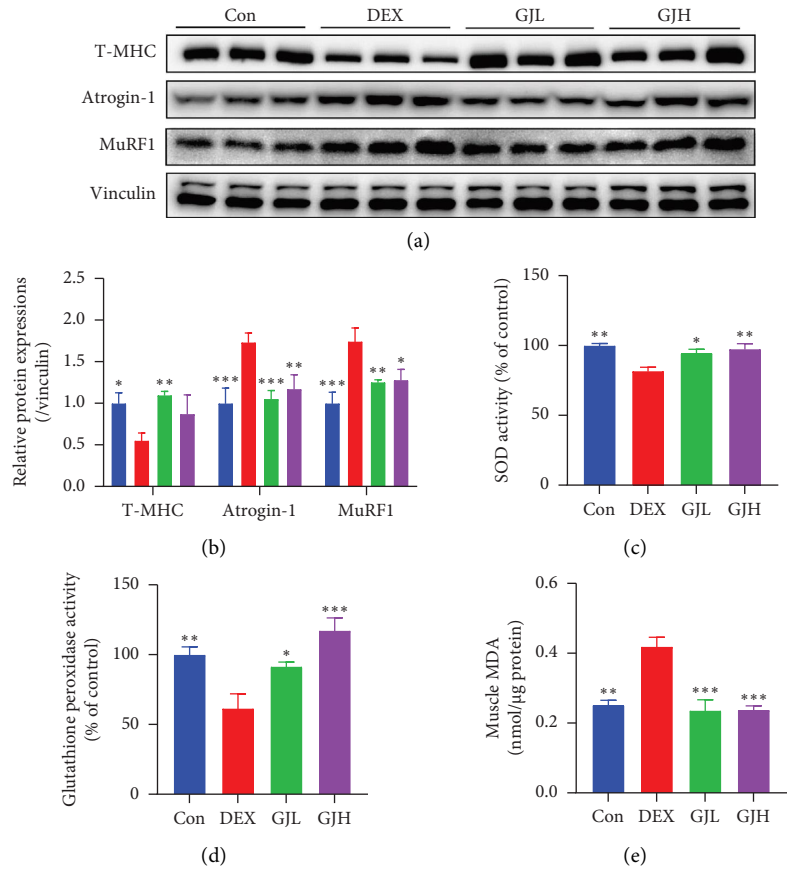
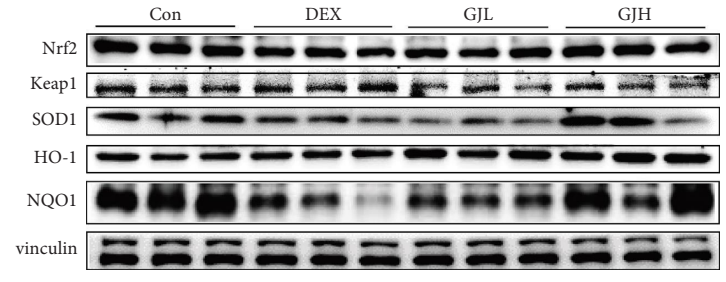
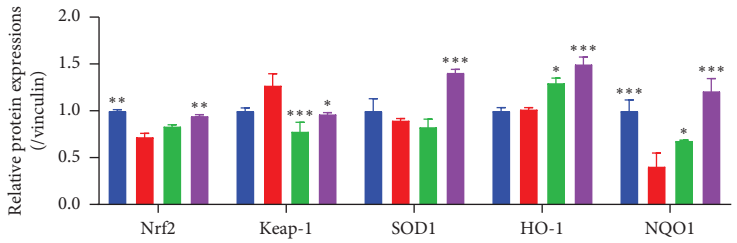


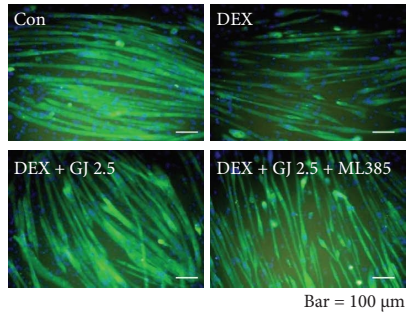
Figure 5: Continued.



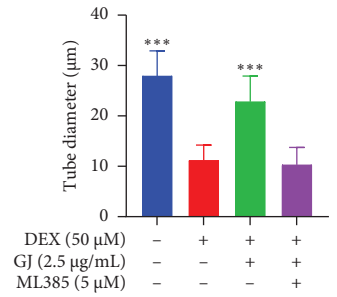
(f)



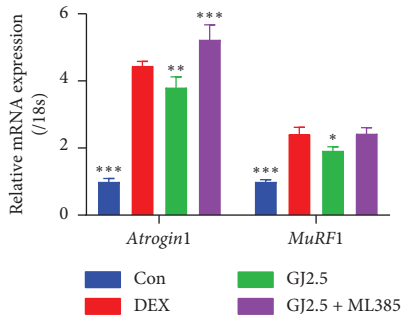
(g)



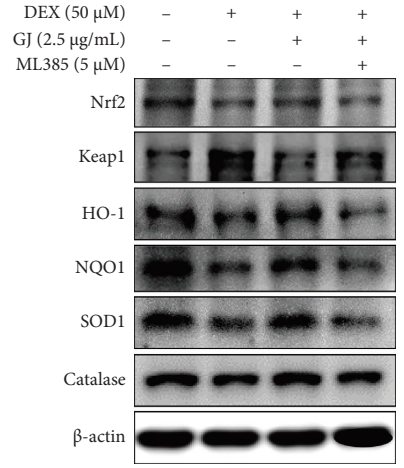
(h)



(i)

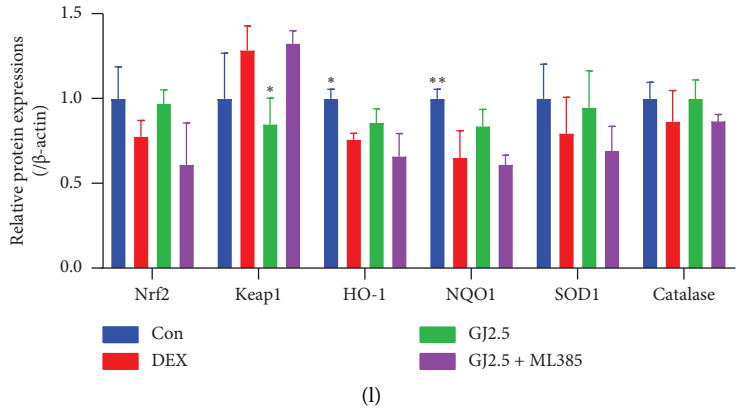


(j)



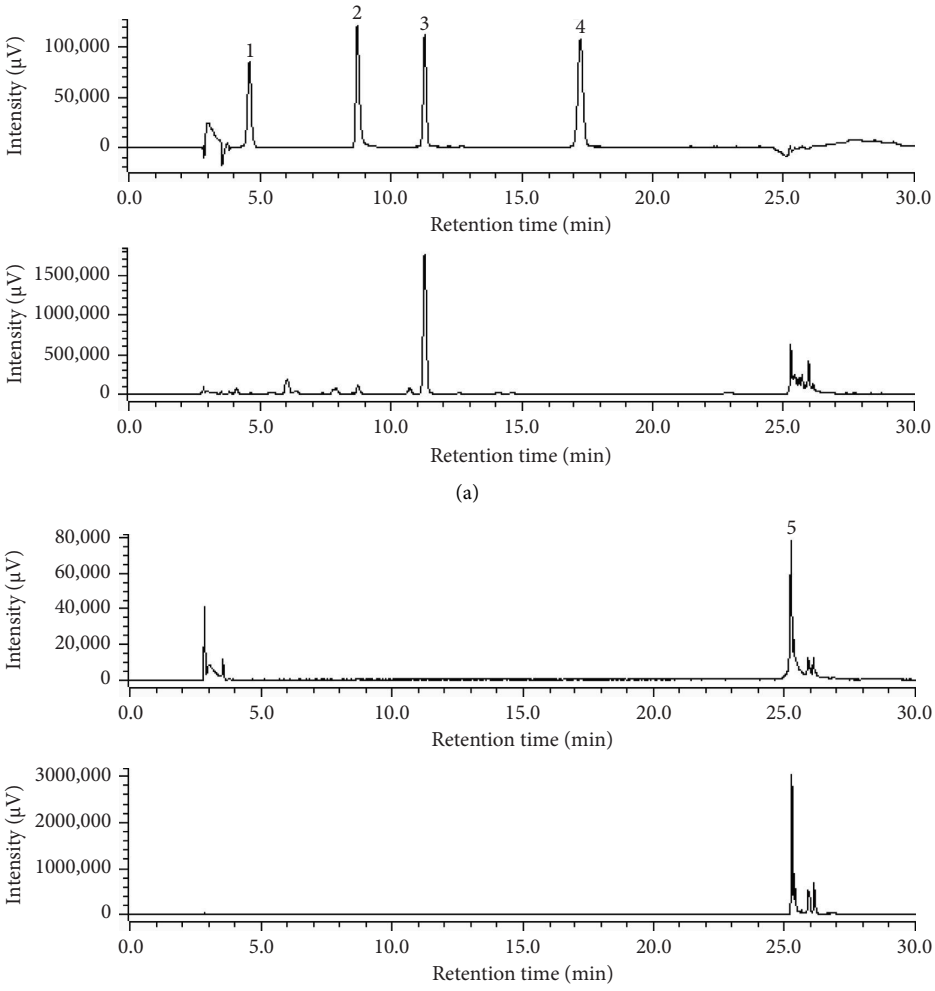
(k)

Figure 5: Continued.



(l)

Figure 5: GJ supplementation reduces oxidative stress of muscle tissue in DEX-induced muscle atrophy via Nrf2 activation. (a) Western blot analysis for total MHC and atrogenes. (b) Quantification of protein bands of (a). (c) Measurement of SOD activity. (d) Glutathione peroxidase activity. (e) The concentration of malondialdehyde (MDA) in muscle tissue. (f) Western blot analysis of Nrf2 and its downstream targets. (g) Quantification of protein bands of (f). (h) IF staining of MHC in C2C12 myotubes. DEX, GJ, and ML385 were cotreated for 24 h. (i) Quantification of myotube diameter. (j) Measurements of mRNA expression (*Atrogin-1* and *MuRF1*). (k) Western blot analysis of Nrf2 and its downstream targets. (l) Quantification of protein bands of (k). Data are means ± SD and SEM. $^{*}p < 0.05$, $^{**}p < 0.01$, $^{***}p < 0.001$ versus DEX.



(a)

(b)

Figure 6: HPLC analysis of the major compounds of GJ extract. (a) Chromatogram at 254 nm for geniposidic acid (1), chlorogenic acid (2), GP (3), genipin (4), and GJ extract. (b) Chromatogram at 450 nm for CC (5) and GJ extract.

Table 1: HPLC analysis of the GJ.

Compound	Retention time (min)	Area	Concentration (mg/g extract)
Geniposidic acid	4.59	98,694	0.87 ± 0.02
Chlorogenic acid	8.69	838,720	6.85 ± 0.09
Geniposide	11.25	15,185,404	135.36 ± 1.55
Genipin	17.23	25,798	0.40 ± 0.01
Crocin	25.21	11,337,163	30.34 ± 0.97

Intake of vitamin E, a known antioxidant, does not increase the lean body mass. Although vitamin E can reduce markers of oxidative damage, its combined supplementation with vitamin C has not been shown to significantly improve muscle thickness or strength in models of age-related muscle atrophy [30]. In addition, dietary antioxidant capacity is not significantly associated with an increase in muscle mass and function in sarcopenia [31]. These findings suggest that the antioxidant capacity to scavenge free radicals may be insufficient to reverse muscle atrophy. In contrast, our findings suggest that CC, a bioactive compound in GJ, not only scavenges ROS but also enhances mitochondrial function and activates the Nrf2 pathway, indicating a more comprehensive mechanism of action beyond simple radical scavenging. Given these mechanistic differences, further investigation is warranted to determine whether GJ and its active components exhibit similar protective effects in clinical settings.

In this study, we found GJ and its active compound CC have radical scavenging activity. Both GJ and CC effectively inhibited mitochondrial ROS production and improved mitochondrial respiration under DEX-induced myotube atrophy conditions. However, it was reported that inhibition of mitochondrial ROS is not enough to rescue muscle atrophy [32], suggesting that additional mechanisms may be involved in the protective effects of GJ and CC against muscle atrophy.

Nrf2 is a transcription factor that counteracts oxidative stress and is negatively regulated by Keap1. One study of Nrf2/Keap1 signaling in aging skeletal muscle found that Nrf2 levels are increased and that those of Keap1 are decreased in older adults who exercise regularly, whereas this pattern was found to be reversed in older adults who were less physically active and sedentary [20, 21]. These findings suggest that Nrf2 could have an important role in the prevention and treatment of muscle atrophy. Previous studies have reported that GJ and CC can stimulate the Nrf2 pathway in various organs and tissues, thereby increasing the antioxidant activity. GJ exhibits protective effects against palmitic acid-induced lipotoxicity through the Nrf2/ARE pathway [33]. Administration of CC protects against chronic obstructive pulmonary disease through the Nrf2 antioxidant system [34]. Moreover, CC improves passive Heymann nephritis, a model that mimics human membranous nephropathy, through the SIRT1/Nrf2/HO-1 signaling pathway [13]. These findings suggest that GJ and CC may also activate the Nrf2 pathway in the muscle tissue, thereby enhancing antioxidant defenses and potentially preventing DEX-induced muscle atrophy.

In this study, GJ induced the upregulation of Nrf2 expression, followed by the downregulation of Keap1 expression. The activation of Nrf2 by GJ results in an increase in the transcription of antioxidant genes encoding SOD, NQO1, and HO-1, which are downstream targets of Nrf2 [22]. NQO1, which is regulated by the transcription factor Nrf2, enhances the antioxidant defenses of cells when its expression is upregulated [35]. Accordingly, our data revealed an increase in NQO1 expression after GJ treatment.

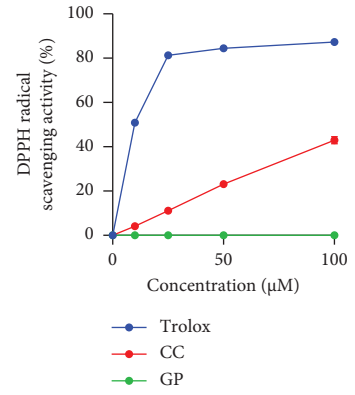
GJ is rich in iridoids and iridoid glycosides, such as genipin and GP. We also confirmed the presence of these compounds in GJ, suggesting that GP and CC are the main functional compounds in GJ. Previously, we reported that GP can protect against DEX-induced muscle atrophy. Moreover, CC has been found to exert anti-inflammatory [36], anticancer [37], and antidepressant [38] effects. However, its preventive effect on muscle atrophy has not been studied. Thus, we studied CC and found that the antioxidant activity of GJ could be attributed to this compound.

Previous study reported that oral administration of GJ extract improved muscle mass and function in a DEX-induced muscle atrophy mouse model [13]. In line with this, our study also demonstrated the ameliorative effect of GJ extract on muscle atrophy and further deepened the mechanistic understanding of its action. Specifically, we found that GJ extract suppressed DEX-induced ROS accumulation and upregulated the expression of antioxidant markers in C2C12 myotubes. Moreover, analysis of CC, the major antioxidant compound in GJ, revealed that CC exerted similar protective effects by reducing ROS levels and alleviating muscle atrophy. By integrating both in vitro and in vivo models, our study complements previous findings and provides clearer insight into the antioxidant-based protective mechanisms of GJ against muscle atrophy.

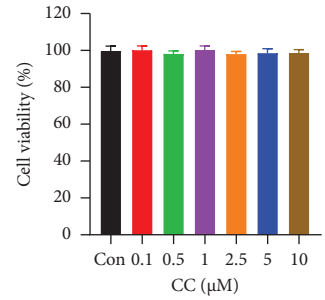
Further validation of CC's specific interaction with antioxidant signaling, future studies employing structure-based approaches such as molecular docking could provide valuable insights into the direct binding interactions between CC and Nrf2-related molecules. Notably, recent studies have shown that natural compounds, including ginsenoside Rc, can exert anti-atrophic effects by directly targeting the glucocorticoid receptor [39, 40]. Such findings underscore the potential of molecular modeling to identify pharmacologically relevant interactions and facilitate therapeutic optimization.

Additionally, considering that muscle atrophy is a multifactorial condition involving not only oxidative stress but also inflammation, mitochondrial biogenesis, and protein degradation pathways such as the ubiquitin–proteasome and autophagy systems, a transcriptome-wide analysis such as RNA-seq could help elucidate the broader spectrum of molecular mechanisms influenced by GJ [41]. This approach may reveal synergistic or pathway-specific actions of other phytochemicals present in GJ beyond CC, thereby deepening our understanding of its therapeutic potential.

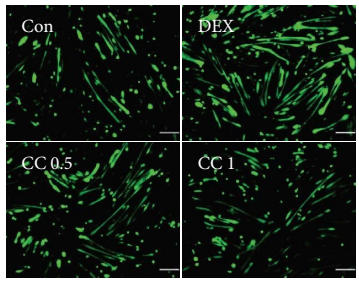
Muscle atrophy is a prevalent condition associated with chronic glucocorticoid use, aging, and sedentary lifestyles, and there is an increasing need for effective yet safe [3].



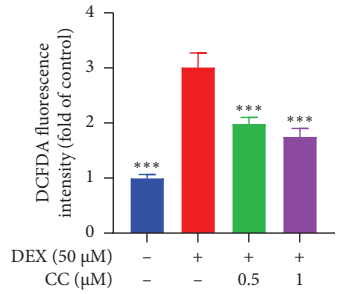
(a)



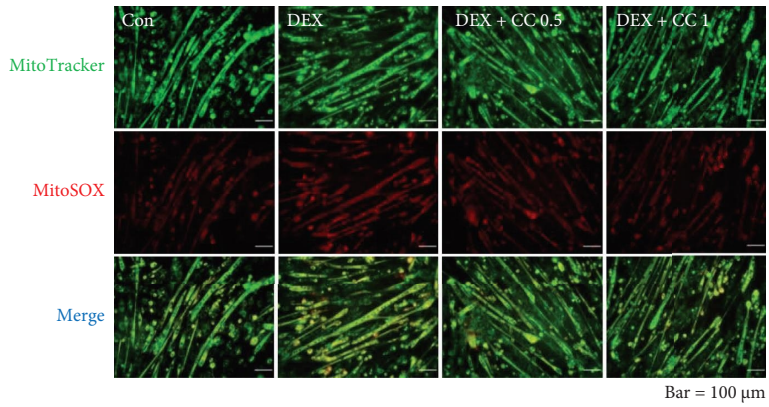
(b)



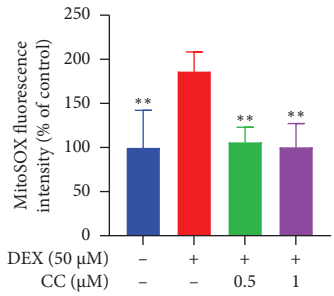
(c)



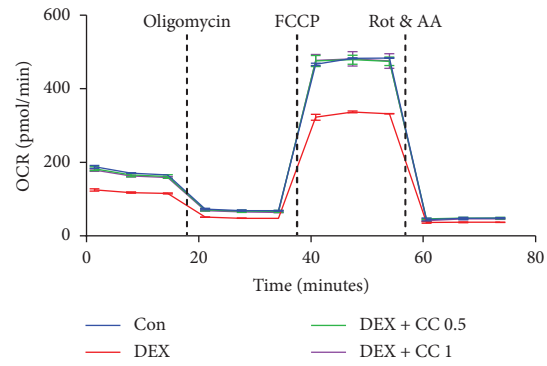
(d)



(e)

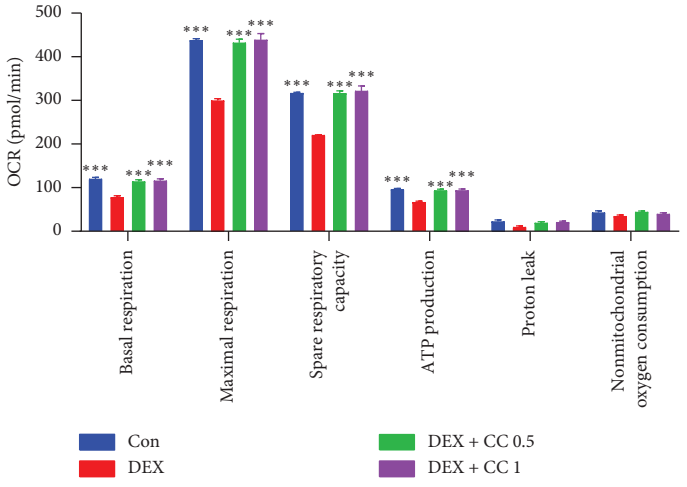


(f)

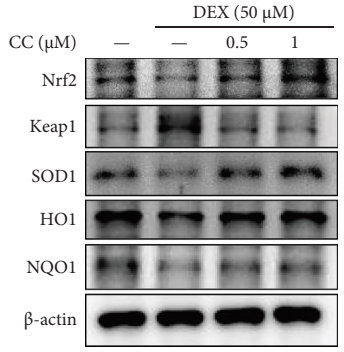


(g)

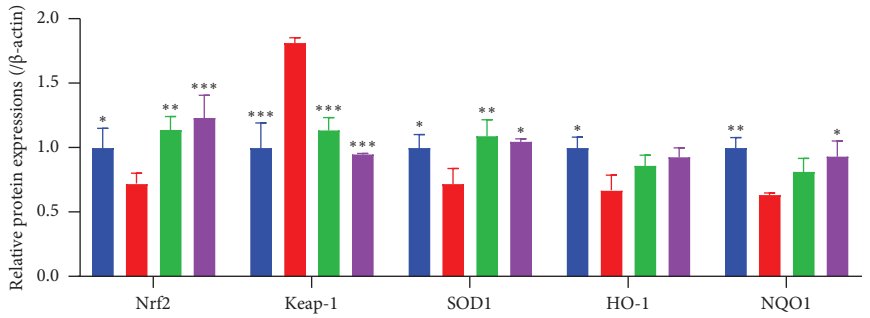
Figure 7: Continued.



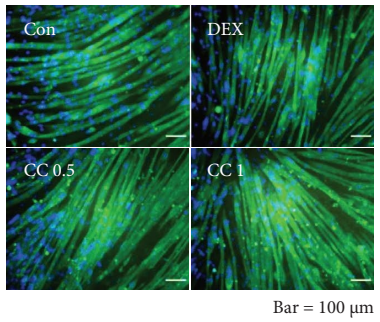
(h)



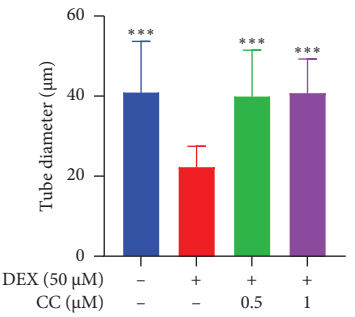
(i)



(j)



(k)



(l)

Figure 7: Continued.

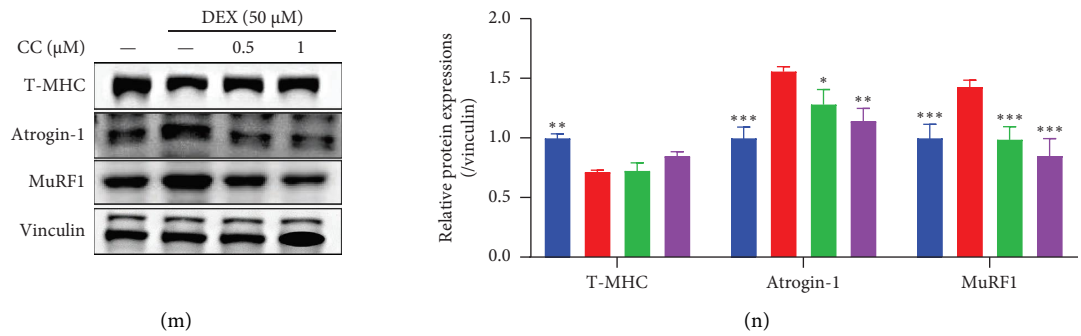


Figure 7: Crocin is the functional component of GJ in DEX-induced muscle atrophy. (a) Comparison of DPPH inhibitory activities of CC and GP (final concentration, 100 μM). (b) Effect of CC on cell viability by MTT assay. (c) Effect of CC on intracellular ROS accumulation in C2C12 myotubes. (d) DCF fluorescence intensity. (e) MitoTracker Green and MitoSOX Red stainings were performed in C2C12 myotubes. (f) Quantification of fluorescent intensity of MitoSOX Red staining. (g) Measurement of OCR. (h) Quantification of mitochondrial respiration. (i) Western blot analysis of Nrf2 and its downstream targets. (j) Quantification of protein bands of (i). (k) IF staining of MHC was performed in C2C12 myotubes. (l) Quantification of C2C12 myotube diameter. (m) Western blotting analysis for total MHC, Atrogin-1, and MuRF1. (n) Quantification of protein bands of (m). Data are means ± SD. $^{*}p < 0.05$, $^{**}p < 0.01$, $^{***}p < 0.001$ versus DEX.

Given its established use as a traditional herbal medicine and favorable safety profile, GJ may serve as a promising candidate for preventive or complementary therapy in managing muscle-wasting conditions. Furthermore, CC, a key bioactive compound in GJ, could be further explored and developed as a natural therapeutic agent targeting oxidative stress-induced muscle atrophy.

5. Conclusion

In this study, we demonstrated that GJ inhibits DEX-induced muscle atrophy by upregulating antioxidant activity through the Nrf2 signaling pathway in both C2C12 myotubes and C57BL/6 mice. GJ increases the expression of proteins related to antioxidants and reduced DEX-induced intracellular ROS accumulation via the activation of Nrf2. Additionally, GJ supplementation enhances tissue antioxidant activity, leading to improved physical performance and an increase in muscle mass. Furthermore, CC, an essential component of GJ, inhibits DEX-induced muscle atrophy by exhibiting intracellular ROS-scavenging activity and activating Nrf2. Therefore, these results underscore the therapeutic potential of GJ and the significance of its functional compound CC as a prospective therapeutic agent for the management of muscle atrophy.

Nomenclature

AREs	Antioxidant response elements
CC	Crocin
CSA	Cross-sectional area
DCF-DA	Dichlorodihydrofluorescein diacetate
DEX	Dexamethasone
DMSO	Dimethyl sulfoxide
DPPH	1,1-Diphenyl-2-picrylhydrazyl
DXA	Dual-energy X-ray absorptiometry
GJ	Gardenia jasminoides
GP	Geniposide
HO-1	Heme oxygenase-1
Keap1	Kelch-like ECH-associated protein 1
MDA	Malondialdehyde
MF20	Anti-MHC mouse monoclonal antibody
MHC	Myosin heavy chain
MTT	3-(4,5-Dimethylthiazol-2-y1)-2,5-diphenyltetrazolium bromide
MuRF1	Muscle-specific RING-finger protein 1
NQO1	NAD(P)H:quinone oxidoreductase 1
Nrf2	Nuclear factor erythroid 2-related factor 2
OCR	Oxygen consumption rate
qRT-PCR	Quantitative reverse-transcription PCR
ROS	Reactive oxygen species
SOD	Superoxide dismutase
TBP	TATA-binding protein

Data Availability Statement

The data that support the findings of this study are available from the corresponding author upon reasonable request.

Ethics Statement

All animal experiments were conducted in accordance with the guidelines of the Institutional Animal Care and Use Committee of the Korea Food Research Institute (Approval No. KFRI-M-19034).

Conflicts of Interest

The authors declare no conflicts of interest.

Author Contributions

Jung-In Kim and **Hang Yeon Jeong:** investigation, data curation, and writing – original draft. **Young In Kim**, **Ahyoung Yoo**, and **Hyunjung Lee:** investigation. **Chang Hwa Jung:** conceptualization and writing – review and editing. **Jiyun Ahn:**

conceptualization, funding acquisition, data curation, writing – original draft, and writing – review and editing.

Jung-In Kim and Hang Yeon Jeong contributed equally to this work.

Funding

This work was supported by the Korea Food Research Institute [grant number KFRI-E0210101].

Supporting Information

Additional supporting information can be found online in the Supporting Information section. *(Supporting Information)*

The primer sequences used for qRT-PCR analysis in this study were provided in Table S1. The standard calibration curves of the analyzed compounds and identification of the CC as the major active compound in GJ are provided in the supporting information (Figures 1S, 2S).

References

[1] W. R. Frontera and J. Ochala, "Skeletal Muscle: A Brief Review of Structure and Function," *Calcified Tissue International* 96, no. 3 (2015): 183–195, https://doi.org/10.1007/s00223-014-9915-y.

[2] E. Volpi, R. Nazemi, and S. Fujita, "Muscle Tissue Changes With Aging," *Current Opinion in Clinical Nutrition and Metabolic Care* 7, no. 4 (2004): 405–410, https://doi.org/10.1097/01.mco.0000134362.76653.b2.

[3] D. J. Wilkinson, M. Piasecki, and P. J. Atherton, "The Age-Related Loss of Skeletal Muscle Mass and Function: Measurement and Physiology of Muscle Fibre Atrophy and Muscle Fibre Loss in Humans," *Ageing Research Reviews* 47 (2018): 123–132, https://doi.org/10.1016/j.arr.2018.07.005.

[4] A. S. Tagliafico, B. Bignotti, L. Torri, and F. Rossi, "Sarcopenia: How to Measure, When and Why," *La radiologia medica* 127, no. 3 (2022): 228–237, https://doi.org/10.1007/s11547-022-01450-3.

[5] L. Larsson, H. Degens, M. Li, et al., "Sarcopenia: Aging-Related Loss of Muscle Mass and Function," *Physiological Reviews* 99, no. 1 (2019): 427–511, https://doi.org/10.1152/physrev.00061.2017.

[6] S. Damiano, E. Muscariello, G. La Rosa, M. Di Maro, P. Mondola, and M. Santillo, "Dual Role of Reactive Oxygen Species in Muscle Function: Can Antioxidant Dietary Supplements Counteract Age-Related Sarcopenia?" *International Journal of Molecular Sciences* 20, no. 15 (2019): 3815, https://doi.org/10.3390/ijms20153815.

[7] G. Bano, C. Trevisan, S. Carraro, et al., "Inflammation and Sarcopenia: A Systematic Review and Meta-Analysis," *Maturitas* 96 (2017): 10–15, https://doi.org/10.1016/j.maturitas.2016.11.006.

[8] K. Sakuma and A. Yamaguchi, "Sarcopenia and Cachexia: The Adaptations of Negative Regulators of Skeletal Muscle Mass," *Journal of Cachexia, Sarcopenia and Muscle* 3, no. 2 (2012): 77–94, https://doi.org/10.1007/s13539-011-0052-4.

[9] L. Yin, N. Li, W. Jia, et al., "Skeletal Muscle Atrophy: From Mechanisms to Treatments," *Pharmacological Research* 172 (2021): 105807, https://doi.org/10.1016/j.phrs.2021.105807.

[10] A. E. Shefrin and R. D. Goldman, "Use of Dexamethasone and Prednisone in Acute Asthma Exacerbations in Pediatric Patients," *Canadian Family Physician Medecin de famille Canadien* 55, no. 7 (2009): 704–706.

[11] C. M. Verhoef, J. A. van Roon, M. E. Vianen, F. P. Lafeber, and J. W. Bijlsma, "The Immune Suppressive Effect of Dexamethasone in Rheumatoid Arthritis Is Accompanied by Upregulation of Interleukin 10 and by Differential Changes in Interferon Gamma and Interleukin 4 Production," *Annals of the Rheumatic Diseases* 58, no. 1 (1999): 49–54, https://doi.org/10.1136/ard.58.1.49.

[12] G. Valesini, R. Priori, A. Francia, et al., "Central Nervous System Involvement in Systemic Lupus Erythematosus: A New Therapeutic Approach With Intrathecal Dexamethasone and Methotrexate," *Springer Seminars in Immunopathology* 16, no. 2-3 (1994): 313–321, https://doi.org/10.1007/BF00197524.

[13] H. Lee, Y. I. Kim, F. S. Nirmala, et al., "Chrysanthemum Zawadskil Herbich Attenuates Dexamethasone-Induced Muscle Atrophy Through the Regulation of Proteostasis and Mitochondrial Function," *Biomedicine & Pharmacotherapy* 136 (2021): 111226, https://doi.org/10.1016/j.biopha.2021.111226.

[14] J. Y. Kim, H. M. Kim, J. H. Kim, et al., "*Salvia plebeia* R.Br. and Rosmarinic Acid Attenuate Dexamethasone-Induced Muscle Atrophy in C2C12 Myotubes," *International Journal of Molecular Sciences* 24, no. 3 (2023): 1876, https://doi.org/10.3390/ijms24031876.

[15] K. Jakubczyk, K. Dec, J. Kałduńska, D. Kawczuga, J. Kochman, and K. Janda, "Reactive Oxygen Species—Sources, Functions, Oxidative Damage," *Polski Merkuriusz Lekarski: Organ Polskiego Towarzystwa Lekarskiego* 48, no. 284 (2020): 124–127.

[16] Y. Kitajima, K. Yoshioka, and N. Suzuki, "The Ubiquitin-Proteasome System in Regulation of the Skeletal Muscle Homeostasis and Atrophy: From Basic Science to Disorders," *The Journal of Physiological Sciences* 70, no. 1 (2020): 40, https://doi.org/10.1186/s12576-020-00768-9.

[17] I. Korovila, M. Hugo, J. P. Castro, et al., "Proteostasis, Oxidative Stress and Aging," *Redox Biology* 13 (2017): 550–567, https://doi.org/10.1016/j.redox.2017.07.008.

[18] F. Campos, J. Abrigo, F. Aguirre, et al., "Sarcopenia in a Mice Model of Chronic Liver Disease: Role of the Ubiquitin-Proteasome System and Oxidative Stress," *Pfluegers Archiv European Journal of Physiology* 470, no. 10 (2018): 1503–1519, https://doi.org/10.1007/s00424-018-2167-3.

[19] H. Hyatt, R. Deminice, T. Yoshihara, and S. K. Powers, "Mitochondrial Dysfunction Induces Muscle Atrophy During Prolonged Inactivity: A Review of the Causes and Effects," *Archives of Biochemistry and Biophysics* 662 (2019): 49–60, https://doi.org/10.1016/j.abb.2018.11.005.

[20] I. Bellezza, I. Giambanco, A. Minelli, and R. Donato, "Nrf2-keap1 Signaling in Oxidative and Reductive Stress," *Biochimica et Biophysica Acta—Molecular Cell Research* 1865, no. 5 (2018): 721–733, https://doi.org/10.1016/j.bbamcr.2018.02.010.

[21] A. Safdar, J. deBeer, and M. A. Tarnopolsky, "Dysfunctional nrf2-keap1 Redox Signaling in Skeletal Muscle of the Sedentary Old," *Free Radical Biology and Medicine* 49, no. 10 (2010): 1487–1493, https://doi.org/10.1016/j.freeradbiomed.2010.08.010.

[22] C. Tonelli, I. I. C. Chio, and D. A. Tuveson, "Transcriptional Regulation by nrf2," *Antioxidants and Redox Signaling* 29, no. 17 (2018): 1727–1745, https://doi.org/10.1089/ars.2017.7342.

[23] I. Bronisz-Budzyńska, M. Kozakowska, P. Podkalicka, N. Kachamakova-Trojanowska, A. Łoboda, and J. Dulak, "The Role of Nrf2 in Acute and Chronic Muscle Injury," *Skeletal Muscle* (2020): https://doi.org/10.1186/s13395-020-00255-0.

[24] T. Hayashi, T. Kudo, R. Fujita, et al., "Nuclear Factor e2-Related Factor 2 (Nrf2) Deficiency Accelerates Fast Fibre Type Transition in Soleus Muscle During Space Flight," *Communications Biology* 4, no. 1 (2021): 787, https://doi.org/10.1038/s42003-021-02334-4.

[25] Y. Chen, H. Zhang, Y. X. Li, et al., "Crocin and Geniposide Profiles and Radical Scavenging Activity of Gardenia Fruits (*Gardenia jasminoides* Ellis) From Different Cultivars and at the Various Stages of Maturation," *Fitoterapia* 81, no. 4 (2010): 269–273, https://doi.org/10.1016/j.fitote.2009.09.011.

[26] B. J. Pyun, J. Y. Lee, Y. J. Kim, et al., "*Gardenia jasminoides* Attenuates Allergic Rhinitis-Induced Inflammation by Inhibiting Periostin Production," *Pharmaceuticals* 14, no. 10 (2021): 986, https://doi.org/10.3390/ph14100986.

[27] T. Tong, M. Kim, and T. Park, "A-Ionone Attenuates High-Fat Diet-Induced Skeletal Muscle Wasting in Mice via Activation of Camp Signaling," *Food & Function* 10, no. 2 (2019): 1167–1178, https://doi.org/10.1039/C8FO01992D.

[28] P. Tangpradubkiat, M. Chayanupatkul, P. Werawatganone, et al., "*Gardenia jasminoides* Extract Mitigates Acetaminophen-Induced Liver Damage in Mice," *BMC Complementary Medicine and Therapies* 24, no. 1 (2024): 371, https://doi.org/10.1186/s12906-024-04676-y.

[29] P. G. Choi, S. H. Park, H. Y. Jeong, et al., "Geniposide Attenuates Muscle Atrophy via the Inhibition of Foxo1 in Senescence-Accelerated Mouse Prone-8," *Phytomedicine* 123 (2024): 155281, https://doi.org/10.1016/j.phymed.2023.155281.

[30] T. Bjørnsen, S. Salvesen, S. Berntsen, et al., "Vitamin C and E Supplementation Blunts Increases in Total Lean Body Mass in Elderly Men After Strength Training," *Scandinavian Journal of Medicine & Science in Sports* 26, no. 7 (2016): 755–763, https://doi.org/10.1111/sms.12506.

[31] A. Aminianfar, R. Hashemi, F. Emami, R. Heshmat, A. D. Motlagh, and A. Esmaillzadeh, "Associations Between Dietary Total Antioxidant Capacity and Sarcopenia: A Cross-Sectional Study," *Nutrition Journal* 23, no. 1 (2024): 87, https://doi.org/10.1186/s12937-024-00933-5.

[32] H. Eshima, P. Siripoksup, Z. S. Mahmassani, et al., "Neutralizing Mitochondrial Ros Does Not Rescue Muscle Atrophy Induced by Hindlimb Unloading in Female Mice," *Journal of Applied Physiology* 129, no. 1 (2020): 124–132, https://doi.org/10.1152/japplphysiol.00456.2019.

[33] H. Ge, J. Li, Y. Xu, et al., "Ameliorative Effect of Fructus Gardeniae Against Lipotoxicity Associated Hepatocytes Injury Through Activating nrf2 Signaling Pathway," *Food Bioscience* 53 (2023): 102596, https://doi.org/10.1016/j.fbio.2023.102596.

[34] M. Dianat, M. Radan, M. Badavi, S. A. Mard, V. Bayati, and M. Ahmadizadeh, "Crocin Attenuates Cigarette Smoke-Induced Lung Injury and Cardiac Dysfunction by Anti-Oxidative Effects: The Role of nrf2 Antioxidant System in Preventing Oxidative Stress," *Respiratory Research* 19, no. 1 (2018): 58, https://doi.org/10.1186/s12931-018-0766-3.

[35] D. Ross and D. Siegel, "The Diverse Functionality of nqo1 and Its Roles in Redox Control," *Redox Biology* 41 (2021): 101950, https://doi.org/10.1016/j.redox.2021.101950.

[36] M. Hashemzaei, C. Mamoulakis, K. Tsarouhas, et al., "Crocin: A Fighter Against Inflammation and Pain," *Food and Chemical Toxicology* 143 (2020): 111521, https://doi.org/10.1016/j.fct.2020.111521.

[37] J. Escribano, G. L. Alonso, M. Coca-Prados, and J. A. Fernandez, "Crocin, Safranal and Picrocrocin From Saffron (*Crocus sativus* L.) Inhibit the Growth of Human Cancer Cells *in Vitro*," *Cancer letters* 100, no. 1-2 (1996): 23–30, https://doi.org/10.1016/0304-3835(95)04067-6.

[38] S. A. Siddiqui, A. Ali Redha, E. R. Snoeck, et al., "Anti-Depressant Properties of Crocin Molecules in Saffron," *Molecules* 27, no. 7 (2022): 2076, https://doi.org/10.3390/molecules27072076.

[39] A. Kim, S. M. Park, N. S. Kim, and H. Lee, "Ginsenoside Rc, an Active Component of Panax ginseng, Alleviates Oxidative Stress-Induced Muscle Atrophy via Improvement of Mitochondrial Biogenesis," *Antioxidants* 12, no. 8 (2023): 1576, https://doi.org/10.3390/antiox12081576.

[40] A. Kim, S. M. Park, N. S. Kim, M. Park, and S. Cha, "Ginsenoside Rc Prevents Dexamethasone-Induced Muscle Atrophy and Enhances Muscle Strength and Motor Function," *Journal of Ginseng Research* 49, no. 1 (2025): 42–52, https://doi.org/10.1016/j.jgr.2024.09.002.

[41] A. Kim, Y. R. Kim, S. M. Park, et al., "Jakyak-Gamcho-Tang, A Decoction of Paeoniae Radix and Glycyrrhizae Radix Et Rhizoma, Ameliorates Dexamethasone-Induced Muscle Atrophy and Muscle Dysfunction," *Phytomedicine* 123 (2024): 155057, https://doi.org/10.1016/j.phymed.2023.155057.